Reference to this paper:

L. Sujbert, Gy. Orosz, " FFT-based Spectrum Analysis in the Case of Data Loss," Proceedings of the IEEE International Instrumentation and Measurement Technology Conference, pp. 800-805, Pisa, Italy, May 11-14, 2015

DOI: 10.1109/I2MTC.2015.7151371

IEEE website: https://ieeexplore.ieee.org/document/7151371

FFT-based Spectrum Analysis in the Case of Data Loss

László Sujbert and György Orosz
Department of Measurement and Information Systems, Budapest University of Technology and Economics
Budapest, Hungary
{sujbert, orosz}@mit.bme.hu

***Abstract*—The significance of measurement data transfer over unreliable channel has emerged in the last decade, due to the spread of sensor networks and the idea of Internet of things. The paper investigates the behavior of the Fast Fourier Transform (FFT) based power spectral density (PSD) estimation in the case of data loss. There are different methods available to estimate the PSD, but the hegemony of the FFT is beyond dispute, especially in real-time applications. The paper investigates the behavior of the PSD estimator in the case of different data loss models, then offers some simple solutions how the data loss can be handled in PSD estimation, when only moderate computing resources are available.**

I. Introduction

Traditional measurement systems provide fast, reliable and high precision data streaming. However, the technological development in the last decade allowed measurement data transfer in much less reliable systems like sensor networks. In this case data can be corrupted or the transmission medium can be partially damaged, etc. [1], [2]. Recently the idea of Internet of things has emerged: the connection of physical things to the Internet makes it possible to access remote sensor data and to control the physical world from a distance [3]. The presence of such systems motivates the investigation of data loss phenomena from signal processing point of view. Our paper deals with one of such measurement problems, the handling of data loss in the case of spectrum estimation.

Two types of methods can be distinguished according to how missing data are handled in spectrum estimation [4]. In the first approach, missing data are estimated using the existing measurements, and traditional spectrum analysis methods are applied on the reconstructed data set. Missing data reconstruction algorithms are ranging from simple sample-and-hold technique [5] to more sophisticated statistical methods [6]. The algorithms can be used either for nonparametric or parametric spectrum estimation like autoregressive modeling [6].

In the second approach, raw data are processed without any reconstruction. Perhaps one of the most famous work in this field is the Lomb–Scargle method [7], [8]. It can handle even irregular sampling, and produces an estimate of the spectrum by least-squares fitting of sine and cosine components with appropriate orthogonalization technique. The Date-Compensated Discrete Fourier-transform (DCDFT) algorithm also uses a kind of sine fitting method on unevenly spaced data [9], and a weight function can be included as well.

Recently the Resonator Based Spectral Observer (RBO) [10] has been adapted to handle data loss. Unlike the aforementioned methods which operate on an entire data record, it estimates the harmonic components recursively. In [11] the conditions for unbiased harmonic estimation are analyzed. An important result is that randomness of data loss can guarantee the convergence. The RBO with its basic settings [10] corresponds to the Discrete Fourier Transform (DFT), which inspired the authors to investigate the behavior of the latter in the case of data loss.

The above mentioned procedures which can recover missing samples or calculate the spectrum based on the available data require much more computational resources than the wide-spread Fast Fourier Transform (FFT). The RBO offers some advantages in real-time applications, but it is still too complicated. The hegemony of the FFT is beyond dispute, especially in real-time applications. The aim of the paper is to offer some simple solutions how data loss can be handled in spectrum estimation, when only moderate computing resources are available. The results are focused but not restricted to measure harmonic signal components.

The paper is structured as follows. Section II recalls the main steps of power spectrum estimation, and Sec. III provides a mathematical description of the problem of data loss. Section IV introduces some data loss models accompanied by their spectral features. In Sec. V a method is proposed that can improve the spectrum estimation in a certain sense. The results are illustrated by simulation results in Sec. VI, while Sec. VII concludes the paper.

II. Power Spectrum Estimation

The technique recalled in this section is well-known, and can be found in many textbooks. The only aim of this overview is to introduce the nomenclature and formulas used throughout the paper. As reference a basic textbook on random data analysis [12] and an eminent paper on windowing techniques [13] can be cited.

The Fourier transform of a sampled signal $x(t_n)$ can be estimated by a finite set of samples as follows [9]:

$$X(f) = \sum_{n=0}^{N-1} x(t_n) e^{-j2\pi f t_n}. \quad (1)$$

Throughout the paper $f \in [0 \ldots 1]$ denotes the discrete frequency, i.e., the frequency relative to the sampling frequency, f_s. The signal $x(t)$ is usually equidistantly sampled, and the spectrum is calculated by the Discrete Fourier Transform

(DFT), thus the formula (1) can be rewritten as:

$$X(f_k) = X(k) = \sum_{n=0}^{N-1} x_n e^{-\jmath \frac{2\pi}{N} nk}, \quad n,k = 0 \dots N-1, \quad (2)$$

where $f_k = \dfrac{k}{N}$ and $x_n = x(t_n)$. The DFT of a signal is usually calculated by the computationally efficient Fast Fourier Transform (FFT). The transformed vector $X(k)$ is generally complex valued, and the spectral content of the signal is expressed by the real valued Power Spectral Density (PSD) function:

$$S(f_k) = S(k) = \frac{1}{N} |X(f_k)|^2. \quad (3)$$

As the PSD is based on a finite set of samples, it can be calculated even for periodic signals. In the case of non-coherent sampling, the estimation suffers from the phenomena of picket fence and leakage. To suppress these effects, windowing techniques have been developed. Windowing means that the signal x_n is multiplied by the so called window function w_n prior to the transform:

$$X_w(k) = \sum_{n=0}^{N-1} x_n w_n e^{-\jmath \frac{2\pi}{N} nk}, \quad n,k = 0 \dots N-1. \quad (4)$$

A huge set of window functions have been developed in the last decades. All of them can improve the result of the estimation, and many of them are optimal in a certain sense.

A significant application of PSD calculation is the analysis of periodic or quasi-periodic signals corrupted by measurement noise. Unfortunately, the measurement noise can hinder the detection of all important harmonic components of the signal. In this case one finite set of N samples is insufficient, a long series of samples are recorded, and many consecutive blocks of N samples are transformed, and the estimator is obtained by averaging the individual PSDs. The blocks can overlap, according to the Welch method. The mean of the individual estimates can be calculated by linear averaging:

$$\bar{S}(k) = \frac{1}{M} \sum_{m=0}^{M-1} S_m(k), \quad (5)$$

where $\bar{S}(k)$ denotes the averaged PSD, and $S_m(k)$ is the PSD of block m. Exponential averaging is also commonly used, when the averaged PSD is calculated in the following way:

$$\bar{S}(k) = \bar{S}(k) + \alpha \left(S_m(k) - \bar{S}(k) \right), \quad (6)$$

where α is the so called smoothing constant, $\bar{S}(k)$ and $S_m(k)$ denote the averaged and the individual PSD, respectively. For high-precision measurements, the bias caused by the noise can be eliminated by subtracting the PSD of the noise from $\bar{S}(k)$.

III. Problem Formulation

A. Formulation of Data Loss

In order to model the data loss, a so called data availability indicator function, K_n, is introduced [15]:

$$K_n = \begin{cases} 1, & \text{if the sample is processed at } n \\ 0, & \text{if the sample is lost at } n \end{cases}, \quad (7)$$

Samples which are not lost will be termed as processed or available samples. Those DFT blocks which don't contain any lost samples will be termed as complete blocks.

The data loss rate can be defined with K_n as:

$$\gamma = \mathbb{P}\text{rob}\left\{ K_n = 0 \right\}, \quad (8)$$

where $\mathbb{P}\text{rob}\left\{\cdot\right\}$ stands for the probability operator. The probability that a sample is available is:

$$\mu = \mathbb{P}\text{rob}\left\{ K_n = 1 \right\} = 1 - \gamma. \quad (9)$$

B. Spectrum Estimation with Missing Data

Equation (1) is a very simple way of spectrum estimation when the sampling is irregular [9]. Hence, this general form can be easily applied for equidistant sampling and missing data, which is a special case of irregular sampling. Equation (1) implies that if a sample is missing, it is not included in the summation (only existing samples are processed). Using the indicator function, K_n, (1) can be rewritten for the case of data loss and equidistant sampling:

$$X(f) = \sum_{n=0}^{N-1} x_n K_n e^{-\jmath 2\pi f n} = \mathrm{DFT}(x_n K_n), \quad (10)$$

This formula means that by incorporating K_n into the usual form of DFT, missing samples are practically substituted with zeros (i.e., their unknown values are multiplied with a zero weight). Mathematically it means that these terms are eliminated from the calculation. Available samples are weighted with $K_n = 1$, which means no modification.

Equation (10) is a very attractive way of spectrum calculation when missing data may exist, since it can be evaluated via FFT.

It is known that (1) often results in biased spectrum estimation for irregular sampling, since basis functions may not be orthogonal [9]. Since the missing data case is a kind of irregular sampling, and (10) is a special form of (1), a bias can also be expected when (10) is used for spectrum estimation. To the best of the knowledge of the authors, no analytical result exist which predict the extent of the bias in this case.

We will analyze what kind of bias can be expected when (10) is used for spectrum calculation when data are missing, and we propose a simple method which can reduce the bias.

The main idea for the analysis of the bias is that in (10), the signal to be transformed is the product of the lossless signal, x_n, and the indicator function K_n. Hence, the PSD of the signal containing missing samples is obtained as the convolution of the PSD of lossless signal (S_x) and the PSD of the data loss indicator function (S_K):

$$S(f) = S_x(f) * S_K(f), \quad (11)$$

where $*$ denotes the convolution operator. The equation shows that a key aspect of the calculation of the PSD of the signal containing missing data is to determine the PSD of the data loss indicator function.

IV. Data Loss Models

In this section, the effect of three basic forms of data loss [5], [14] on the spectrum are investigated:

1) random independent data loss,
2) random block-based data loss,
3) Markov model-based data loss.

The random data loss is one of the most essential data loss models, it is often used because of its simplicity. Block-based data loss models are often used, e.g., when several measurement results are transmitted over packet-based communication systems. When a packet is lost, a whole block of data will be missing from the measurement. Markov data loss models can be used to describe data loss processes when variable length of successive measurement samples are randomly missing.

1) Random Independent Data Loss: Random independent data loss can be defined as follows:

$$\begin{array}{ll} K_n = 1, & \text{with probability } \mu = 1-\gamma \\ K_n = 0, & \text{with probability } \gamma \end{array} \quad \text{for} \quad \forall n. \tag{12}$$

The definition means that each sample is lost with probability γ, and data losses at different time instants are independent of each other.

The PSD of the data loss pattern is:

$$S_K(f) = G + \mu^2 \delta(f), \tag{13}$$

where $\delta(f)$ stands for the Dirac-delta function. Since the values of the indicator function, K_n, are independent at different time instants, they are uncorrelated. Hence, the PSD is white, which is represented by the constant term G. The term $\mu^2\delta(f)$ represents the power of the DC component (i.e., mean value: μ) of the data loss pattern as given in (9). The calculation of G will be considered in subsection IV-A.

2) Random Block-based Data Loss: To define the random block-based data loss, the time axis should be divided into blocks of length M_B. The indicator function is given as:

$$\begin{array}{ll} \{K_{kM_B} \dots K_{(k+1)M_B-1}\} = 1, & \text{with probability } \mu \\ \{K_{kM_B} \dots K_{(k+1)M_B-1}\} = 0, & \text{with probability } \gamma \\ & \text{for } \forall k. \end{array} \tag{14}$$

The definition means that each blocks of length M_B is lost with probability γ, and the data loss in different blocks are independent of each other.

In order to calculate the power spectral density of the data loss pattern, it is considered that this pattern can be constructed as 1 minus the sum of rectangular functions of length M_B. Hence, its PSD can be written as a scaled discrete sinc function plus the mean value of the indicator function:

$$S_K(f) = G \left| \frac{\sin(f\pi M_B)}{\sin(f\pi)} \right|^2 + \mu^2 \delta(f), \tag{15}$$

The frequency of the occurrence of missing blocks determine the total power of $S_K(f)$, which is included in the term G. The calculation of G will be considered in subsection IV-A.

3) Markov model-based Data Loss: The Markov model-based data loss is described by the Markov chain shown in Fig. 1. The states of the Markov chain represent the value of the indicator function K_n. If a sample is available at time instant n, the next sample will be available with probability p, and will be lost with probability $1-p$. If a sample is missing at time instant n, the next sample will be available with probability $1-q$, and will be lost with probability q.

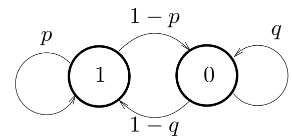

Fig. 1. A two-state Markov model of data loss. State "1": actual sample is available ($K_n = 1$). State "0": actual sample is lost ($K_n = 0$).

The spectral property of a data loss sequence generated by the Markov chain shown in Fig. 1 can be determined according to [16]. Omitting the detailed proof, the PSD of K_n is a first-order, low-pass type spectrum defined as:

$$S_K(f) = G \frac{1}{|1 - az^{-1}|^2} + \mu^2 \delta(f), \tag{16}$$

$$a = p + q - 1, \ \mu = \frac{q-1}{p+q-2}. \tag{17}$$

Again, the calculation of G will be considered in subsection IV-A.

A. Calculation of the Scale Factor

According to the previous subsection, $S_K(f)$ has the general form

$$S_K(f) = Gh(f) + \mu^2 \delta(f), \tag{18}$$

where $h(f)$ determines the spectral shape of $S_K(f)$, and G is an unknown scale factor which will be calculated using Parseval's theorem. The power of the data loss indicator function is calculated from the integral of its PSD i.e., $S_K(f)$, and also from the expected variance of time-domain realization K_n:

$$\int_0^1 \left[S_K(f) - \mu^2 \delta(f) \right] df = \mathbb{E} \left\{ \frac{1}{N} \sum_{i=0}^{N-1} (K_i - \mu)^2 \right\}. \tag{19}$$

For the sake of simplicity, the DC component (μ) is eliminated since it is already known.

Using the fact that $K_n = 1$ for altogether μN samples, and $K_n = 0$ for $(1-\mu)N$ samples, the right hand side of (19) equals to $\mu(1-\mu)$. Hence by substituting (18) into (19), one obtains that:

$$G = \mu(1-\mu) \Big/ \int_0^1 h(f) df, \tag{20}$$

where $h(f) = 1$ for random independent data loss, $h(f) = |\sin(f\pi M_B)/\sin(f\pi)|^2$ for block-based data loss and $h(f) = 1/|1-az^{-1}|^2$ for Markov data loss—see (13), (15) and (16).

B. Effects of Data Loss on PSD

This section discusses what kind of bias is caused by the missing data in the case of a single harmonic signal $x_n = A \cdot \exp(\jmath 2\pi f_0 n)$. The choice is motivated by the fact that all periodic signals can be produced as a superposition of such components. The PSD of $x(t)$ is:

$$S_x(f) = A^2 \cdot \delta(f - f_0). \tag{21}$$

By performing the convolution as given in (11), one obtains the PSD of a signal corrupted by lost samples:

$$S(f) = A^2 \cdot S_K(f - f_0), \tag{22}$$

where $g(x) * \delta(x - x_0) = g(x - x_0)$. Equation (22) means that the PSD of the data loss pattern appears around the frequencies where the periodic signal components are located.

Using the general form (18) one obtains:

$$S(f) = (\mu A)^2 \cdot \delta(f - f_0) + A^2 \cdot Gh(f - f_0) \tag{23}$$

The comparison of (21) and (23) shows that two kinds of bias effects can clearly be distinguished:

1) The estimated amplitude of the signal is decreased by factor μ compared to the original amplitude, A.
2) An extra power, a kind of side lobe, appears around the frequency f_0. The power of the side lobe is proportional to A and G, and its spectral shape is determined by $h(f)$.

V. Improved PSD Estimation

An improved PSD estimation technique should avoid the above mentioned bias and side lobe effects, retaining the resolution of the DFT. In the following a solution is proposed that requires only moderate extra computation.

Suppose that PSD is estimated by the averaging of different data blocks. A straightforward idea to avoid the effects caused by data loss is to use only complete blocks, where no samples are missing. If only complete blocks are used for the estimation, all records containing even only one lost sample are thrown away. A question arises how at least a certain part of such records could be used for the estimation.

The idea is the following: find the first lost data position in the block (if there is any lost sample), and fill the rest of the block by zeros. Then this zero-padded block is used for spectrum estimation. The method can be formulated as follows by the re-definition of the availability indicator function:

$$K_n = \begin{cases} 1 & n = 0 \ldots m_1 - 1 \\ 0 & n = m_1 \ldots N - 1 \end{cases} \tag{24}$$

The indices of the lost samples are denoted by m_i, $i = 1 \ldots M$, i.e. m_1 is the index of the first lost sample in the record. The procedure is demonstrated in Figure 2. Thus the new spectral record is computed in the following way:

$$X(k) = \frac{N}{m_1} \cdot \mathrm{DFT}(K_n x_n) \tag{25}$$

where N is the length of the DFT. The scaling of the spectrum is necessary to compensate for the lost signal power. Zero padding of the signal samples is a well-known procedure to interpolate the spectrum. Indeed, our proposed method is a kind of interpolation, where the number of the original points is variable, depending on the position of the first lost sample. If $m_1 \ll N$, the resolution of the spectral record $X(k)$ is very low. To avoid such a situation, a minimal value $N_{\min}$ of m_1 can be set, and the record is used only if the actual value of m_1 reaches this minimum. Since the length of valid data are between $N_{\min}$ and N, the resolution of the transform is between $\frac{f_s}{N}$ and $\frac{f_s}{N_{\min}}$.

block length,	N	1	256	1024	4096
probability	μ_1	0.999	0.7740	0.3590	0.0166
of complete blocks,	μ_2	0.995	0.2771	0.0059	10^{-9}

TABLE I. Probability of occurrence of complete blocks of different length.

The efficiency of the procedure may be further improved if any uninterrupted part of the block (consisting of at least $N_{\min}$ samples) is also used for DFT calculation. However, in the case of overlapped blocks this selection may result the same time domain data for two consecutive blocks, which is useless for the PSD estimation. Thus the additional improvement of data selection requires further research.

The viability of the idea is illustrated by Table I. Suppose one sample is *not* lost independently of others with a probability of μ_1 or μ_2. The table shows the probabilities that no data are lost for some values of block size. E.g., if a sample is lost with a probability of 0.001, approximately every third block of 1024 samples is complete. However, with the same loss probability, only about one block of 4096 samples out of 60 is complete and can be used for spectral estimation in the usual way. If a 1024 samples long part of a block of 4096 is used for estimation (with zero padding), the settling of the estimator will be approximately 20 times faster.

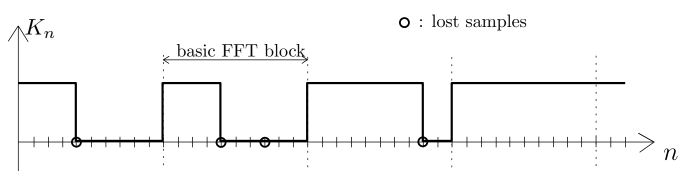

Fig. 2. Modified indicator function of the proposed method.

VI. Simulations

A. Illustration of Bias Effects

First, we demonstrate what kind of bias is caused by missing data in the PSD by the example of a single sine wave.

The parameters of the simulations are: DFT block size is $N = 1024$, data loss rate is $\gamma = 0.001$ ($p = 0.99996$ and $q = 0.96$ in the Markov model), and the PSD $S(f)$ is obtained by averaging the squared absolute value of 1000 DFT blocks calculated according to (10). The signal is:

$$x_n = 2 \cdot \sin(2\pi 0.1 n), \tag{26}$$

i.e., a sinewave with an amplitude of 2 and discrete frequency of 0.1. Actually, the exact frequency was 0.099609 in order to

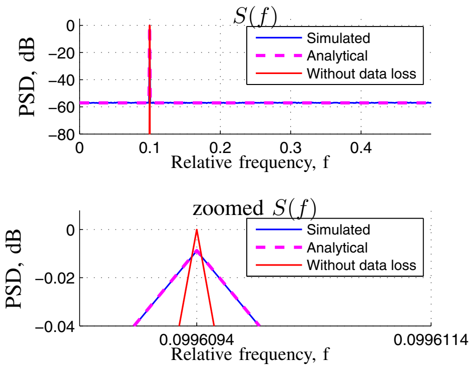

Fig. 3. PSD of signal given in (26). Random independent data loss.

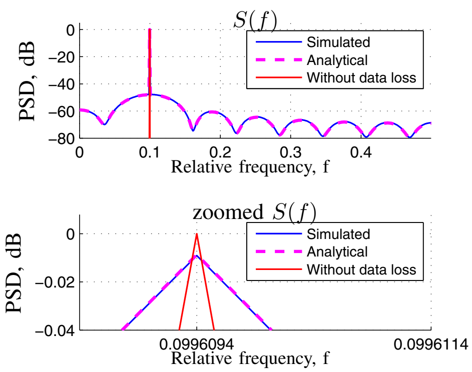

Fig. 4. PSD of signal given in (26). Random block-based data loss.

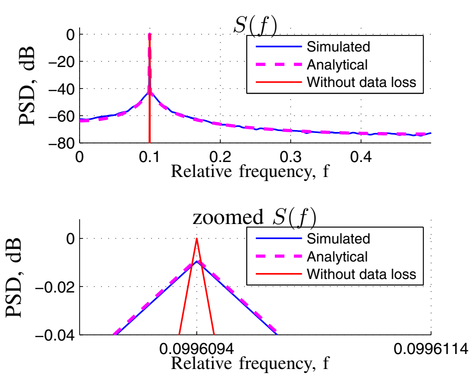

Fig. 5. PSD of signal given in (26). Markov model-based data loss.

ensure coherent sampling, so only the bias caused by data loss can be observed, and no extra bias terms like picket fence or leakage are present.

Fig. 3, 4 and 5 illustrate the two characteristic bias phenomena caused by the data loss. Three kinds of lines are plotted. As a reference, the red line shows $S_x(f)$, i.e., the PSD of the signal if no data were lost. This is a peak at the frequency of the signal, as expected. Blue lines show the PSD calculated by simulations, and dashed magenta lines show the PSD predicted by our analytical models given by (13), (15) and (16).

The top subfigures show the PSDs up to the half of the sampling frequency. One can conclude that side lobes appear around the spectral peak due to the data loss, and these side lobes are correctly predicted by the formulas (13), (15) and (16). The shape of the side lobes are characteristic of the data loss pattern: independent, block-based and Markov data loss patterns result in white, discrete sinc and first-order low-pass-type side lobes, respectively.

The bottom subfigures show the zoomed graphs. They illustrate how the data loss results in the decrease of measured power. As the term $(\mu A)^2$ in (23) shows, in the case of data loss a spectral peak with power $(\mu A)^2$ appears at the frequency of the signal instead of the original power A^2. In the simulations $\gamma = 0.001$, hence $\mu = 1 - \gamma = -0.0087$ dB. Indeed, PSDs obtained from simulations show that the measured powers (blue lines) are a little bit less than 0.01 dB lower than the amplitude of the ideal amplitude (red lines).

B. Complex Example

The effects of data loss and the efficiency of the proposed method is demonstrated by a more complex example. The spectrum of a signal consisting of two sinusoids is estimated. The signal x_n is the following:

$$x_n = \sin(2\pi f_1 n + 0.2\pi) + 0.001 \cdot \sin(2\pi f_2 n + 0.3\pi) \quad (27)$$

where $f_1 = 33/1024$ and $f_2 = 49/1024$. The desired length of the FFT is $N = 1024$, the blocks are not overlapped. To avoid spectral leakage for shorter FFTs, Hanning window is applied. Spectral estimation is performed by exponential averaging of the individual spectra with a smoothing factor of $\alpha = 0.01$. Data loss is modeled by the random independent data loss, with a loss probability of $\gamma = 0.001$. The following table summarizes the settings of the simulation.

FFT length N	overlap	window type	smoothing factor α	data loss rate γ
1024	no	Hanning	0.01	0.001

TABLE II. MAIN DATA OF THE SIMULATION.

The estimated spectra can be seen in Figure 6. The undistorted spectrum is the solid blue curve, while the dashed blue curve belongs to the case when the missing data are replaced by zeros. The spectrum calculated by the proposed method is depicted by solid green line. The spectrum is also calculated using shorter complete blocks, where the length of the FFT was fixed to $N_{\text{short}} = 256$. The result is the dashed green line. Figure 7 zooms to the spectral components of the signal. The figure clearly shows that the second sinusoidal of smaller amplitude is difficult to detect if zeros stand for lost samples (dashed blue line) or shorter FFT is calculated from complete blocks (dashed green line). The proposed method allows the detection of the second component, as well (solid green line). In addition, there is a frequency mismatch of the low resolution spectrum (dashed green line), as the peak of the curve appears at a slightly different position.

Another important feature of the proposed estimation algorithm that its settling is faster. In order to check this, the absolute value of the power estimation is calculated at each step when the estimator is updated. The result for the two important cases can be seen in Figure 8. The settling of the

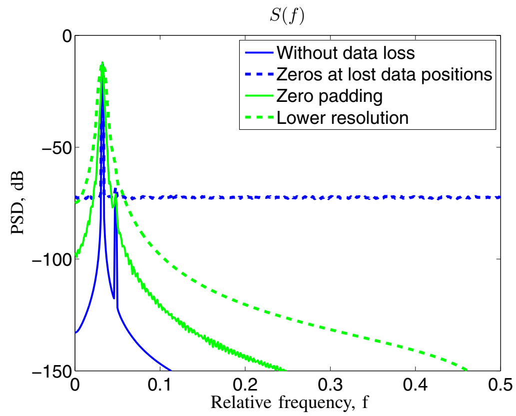

Fig. 6. PSD of the signal given in (27) estimated by different methods.

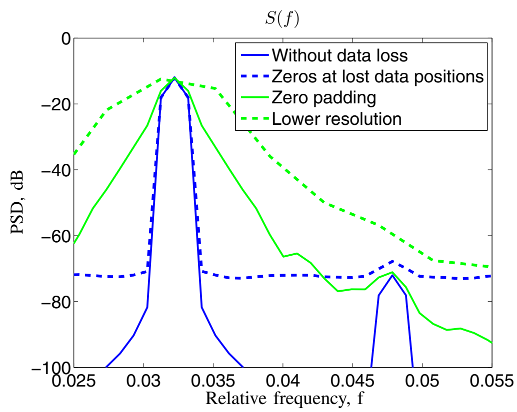

Fig. 7. Zoom on the harmonic components of the signal given in (27).

estimator updated based on complete $N = 1024$ long blocks is plotted by blue circles, while the settling of the proposed estimator represented by green circles. The proposed method outperforms the simple estimator in a convincing manner. The reason is that complete $N = 1024$ long blocks occur with a much less probability than at least $N_{\text{short}} = 256$ long ones as the first row of Table I shows.

VII. Conclusion and Future Work

The paper dealt with the analysis of the FFT based PSD estimation in the case of data loss. Based on prior work, the behavior of the PSD estimator in the case of different data loss models has been investigated. Bias error of the estimation of harmonic components and the spectral leakage due to different data loss models have been calculated. A simple solution has been proposed when only moderate computing resources are available. The simulations show that our method offers faster settling than the obvious ones, mostly retaining the resolution of PSD calculated only by complete records. Extensive comparison with other methods is left for future research, as well as the refinement of the proposed method.

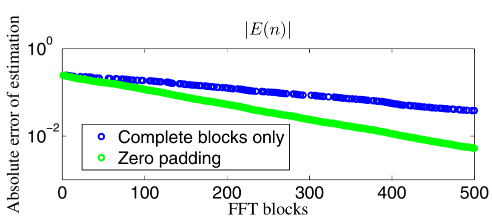

Fig. 8. Settling of two different estimators for the signal given in (27).

Acknowledgment

This work was partially supported by the ARTEMIS JU and the Hungarian Ministry of National Development (NFM) in frame of the R5-COP (Reconfigurable ROS-based Resilient Reasoning Robotic Cooperating Systems) project.

References

[1] L. Kong *et. al*, "Data Loss and Reconstruction in Wireless Sensor Networks," INFOCOM, 2013 Proceedings, Turin, April 14-19, 2013, pp. 1654–1662.

[2] M. Mathiesen, G. Thonet, N. Aakwaag, "Wireless ad-hoc networks for industrial automation: current trends and future prospects," *Proceedings of the IFAC World Congress,* Prague, Czech Republic, July 4-8, 2005, pp. 89–100.

[3] H. Kopetz, *Real-Time Systems,* Springer, 2nd ed., 2011, p. 378.

[4] P. Broersen, S. de Waele, R. Bos, "Application of Autoregressive Spectral Analysis to Missing Data Problems," *IEEE Trans. Instrum. Meas.* Vol. 53, No. 4, July 2004, pp. 981–986.

[5] G. Plantier, S. Moreau, L. Simon, J.-C. Valiere, A. Le Duff, H. Bailliet, "Nonparametric Spectral Analysis of Wideband Spectrum with Missing Data via Sample-and-hold Interpolation and Deconvolution," *Digital Signal Processing* Vol. 22, No. 6, Dec. 2012, pp. 994–1004.

[6] P. M. T. Broersen, S. de Waele, R. Bos, "Estimation of Autoregressive Spectra with Randomly Missing Data," *IMTC2003 - IEEE Instrumentation and Measurement Technology Conference,* Vail, CO, USA, May 20-22. 2003, pp. 1154–1159.

[7] N. R. Lomb, "Least Squares Frequency Analysis of Unequally Spaced Data," *Astrophysics and Space Science* Vol. 39, No. 2, Feb. 1976, pp. 447–462.

[8] J. D. Scargle, "Studies in Astronomical Time Series Analysis. III - Fourier Transforms, Autocorrelation Functions, and Cross-Correlation Functions of Unevenly Spaced Data," *Astrophysical Journal* Vol. 343, Part 1., Aug. 15, 1989, pp. 874–887.

[9] S. Ferraz-Mello, "Estimation of Periods from Unequally Spaced Observations," *Astronomical Journal,* Vol. 86, April 1981, pp. 619–624.

[10] G. Péceli, "A Common Structure for Recursive Discrete Transforms", *IEEETrans. Circuits Syst.* Vol. CAS-33 No. 10. pp. 1035-36, Oct. 1986.

[11] Gy. Orosz, L. Sujbert, G. Péceli, "Analysis of Resonator-Based Harmonic Estimation in Case of Data Loss," *IEEE Transactions on Instrumentation and Measurement,* Vol. 62, No. 2, Feb. 2013, pp. 510–518.

[12] J. S. Bendat, and A. G. Piersol, "*Random Data: Analysis and Measurement Procedures*," John Wiley and Sons, Inc., New York, London, Sidney, Toronto, 1971.

[13] F. Harris, "On the use of Windows for Harmonic Analysis with the Discrete Fourier Transform," in *Proceedings of the IEEE*, Vol. 66 No. 1. pp. 51-83, Jan. 1978.

[14] A. K. Fletcher, S. Rangan, V. K. Goyal "Estimation from Lossy Sensor Data: Jump Linear Modeling and Kalman Filtering," *Proc. of the 3rd International Symposium on Information Processing in Sensor Networks,* Berkeley, California, USA, April 26-27. 2004, pp. 251–258.

[15] B. Sinopoli, L. Schenato, M. Franceschetti , K. Poolla, M. I. Jordan, S. S. Sastry, "Kalman Filtering with Intermittent Observations," *IEEE Trans. on Automatic Control,* Vol. 49, No. 9, Sept. 2004, pp. 1453–1464.

[16] P. Boufounos, "Generating Binary Processes with All-pole Spectra," in *IEEE International Conference on Acoustics, Speech and Signal Processing, 2007. ICASSP 2007.*, Honolulu, HI, vol. 3, 15-20 April 2007, pp. 981-984.